

Komatiites Constrain Molybdenum Isotope Composition of the Earth's Mantle

Nicolas D. Greber^{1,*}, Igor S. Puchtel², Thomas F. Nägler¹, and Klaus Mezger¹

¹*Institute of Geological Sciences, University of Bern, Baltzerstrasse 3, CH-3012 Bern; Tel: +41 31 631 8533*

²*Department of Geology, University of Maryland, College Park, Maryland 20742, USA, Tel: (301) 405-4054*

^{*}*Present address: Origins Laboratory, Department of the Geophysical Sciences, The University of Chicago, 5734 South Ellis Avenue, Chicago, IL 60637, USA*

^{*}Corresponding author. E-mail: greber@uchicago.edu

Abstract

In order to estimate the Mo isotopic composition and Mo abundance in the Bulk Silicate Earth (BSE), a total of thirty komatiite samples from five localities on three continents were analyzed using an isotope dilution double spike technique. Calculated Mo concentrations of the emplaced komatiite lavas range from 25 ± 3 to 66 ± 22 ng/g, and the inferred Mo concentrations in the deep mantle sources of the komatiites range between 17 ± 4 and 30 ± 12 ng/g, with an average value of 23 ± 7 ng/g (2SE). This average value represents our best estimate for the Mo concentration in the BSE; it is identical, within the uncertainty, to published previous estimates of 39 ± 16 ng/g, but is at least a factor of 2 more precise.

The Mo isotope compositions of the komatiite mantle sources overlap within uncertainty and range from $\delta^{98}\text{Mo} = -0.04 \pm 0.28$ to 0.11 ± 0.10 ‰, with an average of 0.04 ± 0.06 ‰ (2SE). This value is analytically indistinguishable from published Mo isotope compositions of ordinary and enstatite chondrites and represents the best estimate for the Mo isotopic composition of the BSE. The inferred $\delta^{98}\text{Mo}$ for the BSE is therefore lighter than the suggested average of the upper continental crust (0.3 to 0.4 ‰). Thus, from the mass balance standpoint, a reservoir with lighter Mo isotope composition should exist in the Earth's mantle; this reservoir can potentially be found in subducted oceanic crust.

The similarity of Mo isotopic compositions between chondritic meteorites and estimates for the BSE from this study indicates that during the last major equilibration between Earth's core and mantle, i.e., the one that occurred during the giant impact that produced the Moon, chemical and isotopic equilibrium of Mo between Fe metal of the core and the silicate mantle was largely achieved.

Keywords: Mo isotopic composition, komatiites, Bulk Silicate Earth, chondritic meteorites, core-mantle equilibrium

1. Introduction

Molybdenum is a redox-sensitive element with a refractory and moderately siderophile character, and, as such, is well suited for studies of chemical differentiation of the Earth ranging from core-mantle differentiation to low temperatures surface processes. Mass-dependent fractionation of stable Mo isotopes has been used for modeling core formation temperatures (Hin et al., 2013; Burkhardt et al., 2014), reconstruction of the extent of past ocean euxinia (e.g., Arnoldt et al. 2004, Pearce et al., 2008; Baldwin et al., 2013) and constraining the timing of the onset of Earth's atmosphere oxygenation (e.g., Wille et al., 2007).

The interpretation of Mo isotopes and their variations in different terrestrial reservoirs is limited by the lack of knowledge of the Mo isotope composition of the Bulk Silicate Earth (BSE). This value is difficult to determine because Mo isotopes can fractionate significantly during magmatic and post-magmatic processes (Voegelin et al, 2014; Greber et al., 2014). Voegelin et al. (2014) showed that amphibole and biotite crystallizing from a silicate melt are enriched in light Mo with $\Delta^{98}\text{Mo}_{\text{melt-mineral}} \geq 0.5 \text{ ‰}$. Furthermore, combined LA-ICP-MS studies and leaching experiments of basalts indicate that magmatic sulfides have on average a higher Mo concentration and a heavier $\delta^{98}\text{Mo}$ than the bulk rock (Voegelin et al., 2012). Thus, even at high-temperatures, Mo isotope fractionation can cause substantial $\delta^{98}\text{Mo}$ heterogeneity within a terrestrial reservoir. Based on the analyses of molybdenites (Greber et al., 2014) and the Mo isotopic data available for igneous continental crustal rocks, an average $\delta^{98}\text{Mo}$ value of 0.3 to 0.4 ‰ is inferred for the Earth's igneous continental crust (Voegelin et al., 2014). While recently published $\delta^{98}\text{Mo}$ values for ordinary, enstatite and most carbonaceous chondrites, as well as iron meteorites, show a homogenous $\delta^{98}\text{Mo}$ of $0.09 \pm 0.02 \text{ ‰}$ (95% confidence interval; n=12), achondrites generally have heavier Mo isotope compositions (Burkhardt et al., 2014). This is consistent with the experimental data suggesting significant Mo isotope fractionation between liquid metal and liquid silicate up to ~2500°C, where the lighter Mo isotopes preferentially enter the metal phase (Hin et al., 2013). On the basis of the Mo isotopic data for chondritic meteorites, Burkhardt et al. (2014) estimated the $\delta^{98}\text{Mo}$ for the BSE between 0.09 and 0.25 ‰. However, direct determinations of the Mo isotope composition of the Earth's mantle have so far not been available.

In this study, komatiites from five different localities from around the globe were investigated in order to better constrain the Mo abundances and Mo isotopic composition of the Archean mantle.

Komatiites are particularly appropriate for this type of study because they are high-MgO volcanic rocks that formed by high degrees of partial melting (~30 to 50%; Arndt, 1977) of the mantle. This melting regime commonly leads to the sampling of large mantle domains, the complete base metal sulfide removal from the residual mantle and the production of sulfur-undersaturated melts (e.g., Keays, 1995). This results in an almost quantitative removal of Mo from the source into the melt and it is therefore expected that the Mo isotope composition of komatiite melts represent the composition of their melting source regions. Komatiite lavas erupted at temperatures of up to 1600°C (Nisbet et al., 1993), which further limits potential Mo isotope fractionation.

2. Samples

A total of thirty komatiite samples from five localities were investigated. Three sample sets come from the Barberton Greenstone Belt in South Africa, and were collected from the lower and upper Komati and the Weltevreden Formations. The upper Komati samples show strong alteration features and were selected to study the effects of alteration on the Mo isotopic systematics. The fourth set comes from the Pyke Hill area in the Abitibi Greenstone Belt (Canada). The fifth set is from the Vetreny Belt in Fennoscandia.

The samples from the different locations represent several chemical types of komatiites that derived from mantle source regions characterized by variable degrees of depletion/enrichment. Those from the lower Komati Formation have Barberton-type $\text{Al}_2\text{O}_3/\text{TiO}_2$ ratios of around 10; their primitive mantle-normalized REE abundance patterns show slight enrichments in light REE and strong depletions in heavy REE (Puchtel et al., 2013). The studied Weltevreden komatiites belong to the Al-enriched type (Connolly et al., 2011) and have primitive mantle-normalized REE patterns exhibiting depletions in light REE and enrichments in heavy REE (Puchtel et al., 2013). The Pyke Hill komatiites belong to the Munro type lavas with $\text{Al}_2\text{O}_3/\text{TiO}_2 \sim 20$. Their primitive mantle normalized REE patterns show depletions in light REE and essentially flat heavy REE abundances (Puchtel et al., 2004b). The komatiites from Victoria's Lava Lake have REE patterns showing enrichment in LREE, which is interpreted to be the result of contamination of the initially LREE-depleted komatiite magma with upper crustal rocks (Puchtel et al., 1996, Puchtel et al., 1997). In order to evaluate the effects of crustal contamination, two tonalite samples (K04, K13) from the Vodla Block, consisting of early Archean

tonalite-trondhjemite-granodiorite complexes thought to underlie the Vetreny Belt lavas (Puchtel et al., 1997), were also analyzed for their Mo concentrations and isotopic compositions.

More information about the samples is given in the Supplementary Material and an overview of sampling details is presented in Table 1.

3. Analytical techniques

3.1. Mo isotope and concentration measurements

For this study, lower Komati Formation and Weltevreden komatiite sample powders prepared by Puchtel et al. (2014), Pyke Hill sample powders from the Puchtel et al. (2004a and 2004b) studies, and the Victoria's Lava Lake and tonalite sample powders from Puchtel et al. (2015) were used. The details of the sample powder preparation techniques are reported in the cited publications. For the upper Komati Formation samples from Tjakastad, altered surfaces were cut off with a diamond saw. The rest of the rock was then cut into small pieces and powdered in an agate disk mill.

Depending on the Mo concentration of the sample, between 0.6 and 2.6 g of material was weighed out into Savillex[®] PFA beakers and spiked with a ¹⁰⁰Mo-⁹⁷Mo double spike. Samples were initially digested for one day in a 5:1 mixture of 22.6 M HF and 14.4 M HNO₃ at room temperature. Then, the sample-acid mixtures were heated in closed beakers to 110°C for ca. 3 days with repeated treatment in an ultrasonic bath. Subsequently they were dried down at 110°C and re-dissolved at 130°C in a 2:1 mixture of 6.4 M HCl and 14.4 M HNO₃ for several days and then dried down again. After this treatment, only chromites were not digested; these chromites were separated from some samples and used for further analyses by LA-ICP-MS. In preparation for the ion exchange chromatography, the solutions were converted into the chloride form via re-dissolution in 6.4 M HCl and drying down again. Molybdenum was then separated from the matrix with a sequential procedure involving anion and cation exchange chromatography, as described by Wille et al. (2007). Depending on the amount of sample material used, more than one anion exchange column step was necessary and each sample was therefore dissolved in the corresponding amount of HCl-H₂O₂. These steps sometimes produced a gel and therefore it was necessary to centrifuge the samples prior to Mo separation. After the anion column chemistry, only one cation exchange chromatography step was

needed to obtain a clean Mo cut. The total analytical blank for Mo was 2 to 3 ng, which corresponds to 2 to 10% of total Mo processed. For several samples (e.g. PH31, 564-5, BV15), however, the blank contribution was as high as 15%. Therefore, 19 out of the 32 samples were replicated with more sample material processed to decrease the blank/sample ratio (up to 80% less blank). All but one analysis (sample BV13) reproduced within analytical uncertainties. In addition, no trend towards heavier or lighter $\delta^{98}\text{Mo}$ values was observed as a function of blank/sample ratios (see Figure S1). Therefore, a strongly fractionated Mo isotope composition of the blank contribution, which would be needed to shift the measured $\delta^{98}\text{Mo}$ values, can be excluded.

The $\delta^{98}\text{Mo}$ compositions were analyzed using a double focusing Nu InstrumentsTM MC-ICP-MS system. The use of a double-spike allowed for the simultaneous determination of the Mo isotope composition and the Mo concentration. Mass-spectrometry routine and double spike calibration are described in detail in Greber et al. (2012). The Mo isotope composition is conventionally given as $\delta^{98}\text{Mo}$ notation:

$$\delta^{98}\text{Mo} = \left(\frac{{}^{98}\text{Mo}/{}^{95}\text{Mo}_{\text{sample}}}{{}^{98}\text{Mo}/{}^{95}\text{Mo}_{\text{reference}}} - 1 \right) \cdot 1000 \quad (1)$$

The data are normalized using the conventional techniques outlined in Nagler et al. (2014), e.g., the $\delta^{98}\text{Mo}$ of NIST SRM 3134 is equal to +0.25 ‰ and mean ocean water has a Mo isotope composition of 2.34 ± 0.07 ‰. This standardization will be used for the discussion throughout this study.

Komatiites have high Ru concentrations, an element that has natural isotopes that have isobaric interferences with ^{100}Mo and ^{98}Mo . Ruthenium was not completely removed by the Mo chemistry and, therefore, corrections for isobaric interferences were applied based on the monitored intensity of the ^{99}Ru peak. More information on the Ru correction, ^{99}Ru signal and $^{99}\text{Ru}/^{95}\text{Mo}$ ratios can be found in the supplementary material and Table S1 and Figure S2. External precision of standard reference material measurements (NIST SRM 3134 and 610, and NIST SRM 612 glasses) was better than ± 0.10 ‰ (2SD; see Greber et al., 2012) and represents the true uncertainty on the measured Mo isotopic ratios, unless stated otherwise. The USGS rock standard SDO-1 processed and analyzed during the same analytical campaign yielded an average $\delta^{98}\text{Mo} = 1.07 \pm 0.05$ ‰ (2SD, n=5), which is in agreement with the suggested value of 1.05 ± 0.14 ‰ (Goldberg et al., 2013).

3.2. LA-ICP-MS; bulk rock chemistry and chromites

Major and trace element concentrations of the two strongly altered Tjakastad samples were determined by XRF and LA-ICP-MS on $\text{Li}_2\text{B}_4\text{O}_7$ glasses. XRF measurements were performed on an Axios, PANalytical wavelength-dispersive X-ray fluorescence spectrometer at the Institute of Geochemistry and Petrology, Department of Earth Sciences, ETH Zürich, Switzerland. LA-ICP-MS was done using an ELAN DRCE quadrupole mass spectrometer (QMS; Perkin Elmer, Canada) coupled with a pulsed 193 nm ArF Excimer laser (Lambda Physik, Germany) and an energy-homogenized (Microlas, Germany) beam profile. Details on the setup and optimization strategies can be found in Pettke et al. (2012). The chromite residua from the sample digestion were collected, placed on thin section slides and chromite grains larger than 40 μm were analyzed using LA-ICP-MS.

4. Results

Molybdenum concentrations and Mo isotopic compositions of the studied komatiite and tonalite samples are presented in Table 1.

The Mo concentrations of the komatiites from the lower Komati Formation range from 13 to 51 ng/g and the $\delta^{98}\text{Mo}$ values range from 0.11 ± 0.10 to 0.69 ± 0.10 ‰. The $\delta^{98}\text{Mo}$ and the Mo concentrations correlate well with each other and with the indices of magmatic differentiation (Figures 1A, 2 and 3). The Mo concentrations correlate negatively with elements compatible in olivine, such as MgO and Ni (Figures 1A and 2D), and positively with the incompatible elements, such as Al_2O_3 and TiO_2 (Figure 2A and 2B). The $\delta^{98}\text{Mo}$ values show negative correlations with the Mo concentrations and positive with the MgO concentrations (Figure 3). Molybdenum concentrations correlate with Pt (Figure 2C) and Pd. The sample from the chilled margin (BV02) has the highest Mo concentration and the lightest $\delta^{98}\text{Mo}$, ~ 0.18 ‰ lighter than the olivine cumulate from the same lava flow (BV01).

The Mo concentrations of the samples from the Weltevreden Formation range from 9 to 30 ng/g. The Mo isotope compositions range from -0.04 ± 0.10 to 0.13 ± 0.10 ‰ (Figure 4). The Mo concentration of the lava flows SA501 and KBA12 correlate negatively with MgO (Figure 1B) and Ni (Figure 2D) and positively with the elements that are incompatible in olivine (e.g. Al_2O_3 , TiO_2 , Pt, see Figure 2). The only two samples from flow SA564 analyzed (i.e. 564-4 and 564-5) have lower Mo concentrations that plot below these trends (see Figures 1B and 2), which may indicate Mo mobility

during postmagmatic processes. This is at odds with the Re behavior in these samples, which shows no evidence for disturbance (Connolly et al., 2011; Puchtel et al., 2014).

The Mo concentrations of the samples from the Pyke Hill komatiites range from 18 to 46 ng/g and show the same correlations with geochemical parameters as observed in the other two komatiite locations. The $\delta^{98}\text{Mo}$ values span a very narrow range between $-0.07 \pm 0.10 \text{ ‰}$ and $0.17 \pm 0.10 \text{ ‰}$ (Figure 4) and do not correlate with other geochemical parameters.

The Mo concentrations of the Victoria's Lava Lake samples are the highest among the studied komatiites and range from 114 to 256 ng/g. The $\delta^{98}\text{Mo}$ values range between 0.06 ± 0.10 and $0.32 \pm 0.10 \text{ ‰}$. There is no correlation between the Mo isotope composition and the lithology within the lava lake or any available geochemical data. The Mo concentrations exhibit, as expected, negative correlations with elements compatible in olivine (Figures 1E and 2D) and positive correlations with incompatible elements (Figures 2A and 2B).

The two analyzed Tjakastad samples from the upper Komati Formation have high SiO_2 , Na_2O , Al_2O_3 and low MgO and Ni concentrations, indicating that these rocks were strongly altered. The Mo isotope compositions and Mo concentrations are similar in both samples, at around 0.70 ‰ and 81 ng/g, respectively. Major and trace element concentrations of these samples are given in Table S2.

5. Discussion

5.1. General considerations

5.1.1. Chromites

Due to their high resistance to acid attack, chromites were not completely digested during the chemical procedures applied, which potentially resulted in an analytical bias in determining the Mo isotopic composition and concentration in the samples. In order to evaluate the effect of undigested chromites on the bulk rock Mo concentration and isotope composition, chromites from several komatiite samples were analyzed for their Mo concentration by LA-ICP-MS. The major element compositions of these chromites were also analyzed and are reported in Table S3; these are similar to those reported in Puchtel et al. (1996). The Mo concentrations in the chromites determined by LA-ICP-MS are below the detection limit, except for some chromite grains in sample 91111 from Victoria's Lava Lake. Calculating a Mo partition coefficient (K_d) based on the Mo concentration in sample 91111 gives a $K_{d\text{chromite-melt}} = 11$. Using this value and an assumption that all Cr in the sample is present in

chromite, it is calculated that the Mo contribution of the chromites to the total Mo inventory in the bulk rock is less than 5%. This value can be considered a maximum estimate, and was likely much less, since there are also other minerals in the studied samples that contain Cr, such as olivine and orthopyroxene. Although olivine is not a major host of Cr ($K_{d_{Ol-melt}}$ for Cr is around 0.7: Adam and Green 2006), orthopyroxene is ($K_{d_{Opx-melt}}$ around 8: Adam and Green 2006). Based on these considerations, we conclude that the undigested chromites likely had a negligible effect on the measured bulk rock Mo isotope compositions and concentrations.

5.1.2. Alteration and magmatic Mo isotope fractionation

Since Mo species are soluble in water under oxidizing conditions, Mo might have been mobilized during secondary alteration. Thus, it is essential to consider the influence of alteration processes on the Mo isotope composition and concentrations. A commonly used technique to evaluate mobility of an element in komatiitic rocks is to plot this element against indices of magmatic differentiation, such as MgO content, and evaluate if its abundances plot on olivine control lines (Arndt et al., 1977). This approach uses the fact that the only major liquidus phase in komatiitic magmas over a wide range of temperatures and pressures is olivine (Arndt, 1976). This approach is shown in Figure 1 for the samples investigated here. If Mo concentrations were unaffected by secondary alteration, the olivine control line drawn through the Mo vs. MgO data should intersect the MgO-axis at the average MgO concentration of the olivine in equilibrium with the emplaced komatiite lava.

Here, we used the published MgO concentrations in olivines from the studied komatiite suites. The MgO vs. Mo regression line for Victoria's Lava Lake intersects the MgO-axis close to the average MgO content of the liquidus olivine in this system (i.e., ~48 wt.%, Puchtel et al., 1996), demonstrating immobile behavior of Mo during secondary alteration of this komatiite suite (Figure 1E).

For the Weltevreden komatiite suite, when omitting samples from lava flow SA564 (i.e., 564-4 and 564-5), the regression line through the other samples intersects the horizontal axis at the MgO concentration of olivine from that locality (i.e., ~54 wt.%, Puchtel et al., 2013; Figure 1B). This suggests pristine Mo signatures for rock samples of lava flows SA501 and KBA12, but potentially lower Mo content in the samples from lava flow SA564 due to alteration. As there is no obvious difference in the Mo isotope composition between flow SA564 and the other two flows, the $\delta^{98}\text{Mo}$ seems to be unaffected by the alteration process at this locality.

The Mo concentrations of the Pyke Hill komatiite samples show a good correlation with the MgO content; however, samples plot on a regression line with a slope that is steeper than that of the olivine control line, indicating some Mo mobility in the cumulate samples, in-line with the observation of some limited mobility of Re in the same cumulate samples (Puchtel et al., 2004b). Nonetheless, all Pyke Hill komatiites have very similar and consistent $\delta^{98}\text{Mo}$ values indicating that alteration processes affected Mo in the Pyke Hill samples only to a small degree, if at all. Regressions using the samples with the highest (PH14) and lowest (PH13) Mo concentration through the pre-defined olivine MgO concentration of ~52 wt% (Puchtel et al., 2004a) are used to calculate the concentrations of Mo in the emplaced komatiite lava and the mantle source of the Pyke Hill komatiites (Figures 1C-D).

The lower Komati Formation komatiites are the samples showing the biggest range in their Mo isotope compositions within the same locality (see Figure 3 and 4). Even though these rocks are well preserved by Archean standards, they were still modified by seafloor alteration and metamorphism (Puchtel et al., 2013). Although Mo concentrations show a good correlation with the MgO content, the data plot on a trend with a slope steeper than that of olivine control line (Figure 1A). This implies either (a) mobile behavior of Mo during seafloor alteration and/or metamorphism or (b) Mo concentrations and $\delta^{98}\text{Mo}$ were influenced by magmatic fractionation or mantle source heterogeneity.

If alteration or metamorphism were significant, these processes have to account for the observation that the lower Komati Formation is the only studied location that exhibits significant Mo isotope variations and in addition, a correlation between the $\delta^{98}\text{Mo}$ and MgO concentration. The heaviest $\delta^{98}\text{Mo}$ of the lower Komati Formation (BV15 = 0.69 ± 0.10 ‰) is similar to the Mo isotope composition of the strongly altered and geographically closely related Tjakastad samples from the upper Komati Formation (average of 0.70 ± 0.10 ‰; Figure 4 and Table 1). This similarity might indicate that the Mo isotope compositions of the lower Komati samples are modified by alteration, whereby the samples with the lowest Mo concentrations are affected the most. A Mo isotope shift towards a heavier composition is in line with the observations about the behavior of Cr isotopes during weathering of ultramafic rocks (Farkaš et al., 2013). Even though Cr is not necessarily concentrated in the same minerals as Mo, both are redox sensitive elements, soluble under oxidizing conditions, and they form similar complexes under Eh and pH conditions of surface waters (i.e. MoO_4^{2-} , HMoO_4^- , H_2MoO_4 vs. CrO_4^{2-} , HCrO_4^- ; Oze et al., 2007). Thus, Cr can serve as the first order analogue for Mo in these environments and during surface alteration of ultramafic rocks. Puchtel et al. (2014) provided

evidence that Re was mobile during alteration in these ultramafic rocks. This led to significant scatter in a Re vs. MgO diagram. As Re behaves geochemically similar to Mo, the striking correlation between Mo concentrations and $\delta^{98}\text{Mo}$ with, e.g., MgO contents (Figure 3) is inconsistent with the suggestion that the Mo signature was modified by alteration. It rather indicates that the Mo concentrations obtained for these samples are most likely primary. If alteration or metamorphism cannot account for the variability of the Mo isotopes in the komatiites of the Komati Formation, then magmatic processes need to be considered.

High temperature Mo isotope fractionation in magmatic and hydrothermal systems has been observed and described in the literature, as has been outlined in the introduction. Silicate minerals, such as amphibole and biotite, have been shown to preferentially incorporate lighter Mo isotopes during crystallization in subduction-related magma chambers (Voegelin et al., 2014), leaving behind a melt enriched in isotopically heavy Mo. In addition, combined LA-ICP-MS measurements and leaching experiments of basalts revealed compatible behavior of Mo in early magmatic sulfide melt inclusions that are also hosts for heavier Mo isotopes (Voegelin et al., 2012). If igneous processes dominated the Mo signatures of the lower Komati Formation, the observed Mo concentrations and isotope compositions, as well as major and trace element compositions of these rocks, should show predictable trends.

Since Mo isotope compositions are heavier in samples with higher MgO concentrations (early precipitates), this implies that an early cumulate phase should have incorporated Mo with a $\delta^{98}\text{Mo}$ heavier than that of the melt. Silicate minerals, however, are inferred to incorporate lighter Mo isotopes, at least in systems with higher oxygen fugacity, a parameter that can influence the speciation of Mo and other elements and thus has an effect on the isotope fractionation of redox sensitive elements in general (see Dauphas et al., 2014). The V partitioning behavior between olivine and komatiite melt in the lavas from the lower Komati Formation and Weltevreden Formation indicates that these two komatiite systems differentiated under similar $f\text{O}_2$ (Puchtel et al., 2013); however, their range of Mo isotope fractionations is different. This observation is inconsistent with $f\text{O}_2$ being the dominant factor of Mo isotope fractionation in these rocks. Fractionation of sulfide minerals or immiscible sulfide liquid cannot explain the observed pattern either. The main argument against this possibility is that highly siderophile elements, such as Pt and Pd, that have a stronger affinity for sulfide phases than Mo, plot on olivine control lines (Puchtel et al., 2014) and, therefore, do not show

any evidence for fractionation of significant amounts of sulfides. In addition, experimentally determined Mo partition coefficients between sulfide phases and silicate liquid indicate that small amounts of sulfides do not strongly influence the Mo concentration of the silicate melt (Li and Audétat, 2012). Not much is known about the partitioning behavior of Mo in oxides. Chromite is the most common oxide phase fractionating in komatiite lavas when the MgO content of the liquid drops below 24% (Barnes, 1998). However, Cr₂O₃ concentrations in the samples from the lower Komati formation differ only by \pm 0.03 wt. %. Since chromites contain between 50 and 60 wt% Cr₂O₃ (Table S3), only ca. 0.06% chromite is needed to account for the differences in the Cr concentrations among the samples. This small amount of chromite cannot account for the observed variations in the Mo isotopic compositions, unless the Mo partition coefficient between chromite and silicate melt is significantly higher compared to those obtained for the Weltevreden and Victoria's Lava Lake suites.

Another hypothesis would be that the Mo isotope fractionation occurred just after komatiite lava emplacement, but prior to its solidification. Samples BV01 and BV02 are from the same lava flow. Even though their $\delta^{98}\text{Mo}$ are within error identical, the olivine cumulate sample BV01 follows closely the trend for the other cumulates towards a heavier $\delta^{98}\text{Mo}$. Sample BV02 is likely to be the one that best represents the primary lava compositions, because it is a chilled margin sample and, as such, had not experienced any substantial fractional crystallization. On this basis, an olivine control line can be drawn through the composition of this sample and that of the earliest olivine precipitates. Using this olivine control line, the deviation between the Mo concentrations of the samples and those predicted can be calculated for each analyzed sample. Using a Rayleigh distillation model, a very homogeneous $\delta^{98}\text{Mo}$ fractionation of -0.41 ± 0.03 ‰ (2SD) can be estimated and a perfect fit through all data points is achieved (see Figure 5 and Table S4). This result indicates that the initial lavas from all flows could have been almost identical in their Mo concentrations and isotope compositions. A process during lava emplacement removing light Mo isotopes prior to crystallization of the komatiite rocks thus might account for the observed isotope variations and the steeper Mo vs MgO trend. The fractionating phase could be a Mo bearing mineral or metal alloy that was sequestered right after lava emplacement and was not sampled by the rocks investigated.

Alternative causes for the correlation of Mo isotopes with higher MgO could be mantle source heterogeneity and/or dynamic melting during the ascent of a plume, similar to what has been suggested for the Gorgona komatiites (Arndt et al., 1997). Indeed, Puchtel et al. (2013) argued for a

decrease in trace element concentrations in the studied komatiite lava flows from the bottom of the lava sequence upwards, which caused steepening of the MgO vs trace element trends when samples from across the lava sequence were plotted together. Both, mantle source heterogeneity or observation that succeeding komatiite lava flows were generated from progressively more depleted mantle domains within the same rising mantle plume, could account for the fractionated Mo signature of the lower Komati Formation komatiites. In this latter model, depletion of the lower Komati Formation mantle source results in lower Mo content but enrichment of heavy isotopes. The strength of this hypothesis is that it explains the steep Mo vs. MgO trend, the good correlation between $\delta^{98}\text{Mo}$ and MgO, as well as the decrease in other trace element concentrations from the bottom of the lava sequence upwards observed by Puchtel et al. (2013).

At this stage, no conclusive answer can be given as to which of the processes was most likely responsible for the observed Mo signature in the lower Komati Formation samples. Regardless of the specific mechanism that was responsible for the variations in the Mo isotopic compositions of the Komati lavas, chilled margin sample BV02 represents best the Mo isotopic composition of the emplaced komatiite lavas. Therefore, further calculations and interpretations regarding this komatiite suite will use the data for this sample only.

5.2. Molybdenum concentrations and isotope compositions of the komatiite lavas

The Mo concentration of the emplaced komatiite lavas can be estimated from the MgO vs. Mo regressions for samples from a given locality and using the published calculated MgO content of the emplaced komatiite lava from Puchtel et al., (1996), Puchtel et al., (2004a), Connolly et al. (2011) and Puchtel et al., (2013). The MgO concentrations of the emplaced lavas at the lower Komati and Weltevreden Formation komatiites are 29.4 ± 0.3 wt. % and 31.4 ± 0.9 wt. %, respectively (Connolly et al. 2011, Puchtel et al., 2013). The MgO concentration of the primary komatiite lava at Pyke Hill has been shown to be 27.4 wt. % (Puchtel et al. 2004a). The emplaced komatiite lava at Victoria's Lava Lake had a MgO concentration of 14.8 wt. % (Puchtel et al., 1996). The calculated primary Mo concentrations of the emplaced komatiite lavas, using either olivine control lines or fitted regressions, are 33 ± 8 ng/g for Pyke Hill, 25 ± 4 ng/g for Weltevreden, and 51 ± 6 ng/g for the lower Komati locality.

For the Weltevreden and lower Komati Formations, an estimated uncertainty on the regression was used to calculate the maximum and minimum Mo concentrations at the limits of the MgO concentrations of the emplaced komatiite lava (see Figure 1). The estimated error on the primary Mo concentration of the lower Komati Formation is ± 5 ng/g, resulting from a 10% uncertainty on the Mo concentration of sample BV02. The error on the primary Mo concentration of the emplaced komatiite lava at the Weltevreden locality has been defined using the error estimate on the Mo concentration from the MgO vs. Mo regression, i.e., ± 2.5 ng/g. For the Pyke Hill komatiites, a maximum (sample PH14) and minimum (sample PH31) regression through the pre-defined MgO concentration of olivine were used to estimate the uncertainties (Figure 1).

The original komatiite melt from Victoria's Lava Lake assimilated around 8% of crustal material *en route* to the surface (Puchtel et al., 1996). Since the material of the continental crust is estimated to contain ca. 800 ng/g Mo (Rudnick and Gao, 2003), crustal contamination must have resulted in the increase in Mo concentrations in the emplaced Vetreny komatiite lava. In order to calculate the Mo content in the original Vetreny komatiite magma, the contribution from the crustal contaminant first needs to be accounted for. Two tonalites from the Vodla block, which were expected to represent the contaminant, were analyzed for their Mo concentrations and isotope compositions. The Mo concentrations of the tonalites range from 15 to 46 ng/g (Table 1), which is even lower than those obtained for the Victoria's Lava Lake komatiites. This implies that either this particular samples lost a substantial amount of their Mo inventory after emplacement of the komatiites, or that these samples are not representative for the composition of the contaminant in terms of their Mo content. Therefore, the estimated Mo content of the bulk continental crust of 800 ng/g (Rudnick and Gao 2003) is used to account for the effects of crustal contamination. Based on the well-defined MgO vs. Mo correlations in the Vetreny lava lake, the contaminated komatiite lava upon emplacement is calculated to contain 175 ± 18 ng/g Mo. To account for the effects of olivine fractionation prior to lava emplacement, the Mo concentration in the inferred original komatiite lava with 25 ± 2.5 wt% MgO (Puchtel et al., 1996) was calculated using the composition of the actual emplaced komatiite lava with 14.8% MgO and 175 ± 18 ng/g Mo and the estimated liquidus olivine composition with 50 wt.% MgO in equilibrium with the original komatiite (Puchtel et al., 1996). This results in a Mo concentration of 125 ± 18 ng/g for a komatiite lava with ~25 wt% MgO. From this value, the effects of $8 \pm 1\%$ crustal contamination were

subtracted, which yields a Mo content of 66 ± 22 ng/g for the original, uncontaminated melt of the Victoria's Lava Lake komatiites.

The estimated 8% contamination with the continental crustal material results in $62 \pm 13\%$ of the Mo inventory in the Victoria's Lava lake komatiite being derived from that of the contaminant. The $\delta^{98}\text{Mo}$ value of 0.17 ± 0.07 ‰ obtained for the Victoria's lava lake komatiites is, therefore, dominated by the Mo isotopic composition of the contaminant. Although the Mo isotopic composition of the bulk continental crust has not yet been defined. Voegelin et al. (2014) suggested that the upper continental crust had a $\delta^{98}\text{Mo}$ of around 0.3 ± 0.1 ‰. As such, this value is used to account for the effect of crustal contamination on the Mo isotopic composition of the original komatiite magma. Our calculations yield $\delta^{98}\text{Mo}$ of -0.04 ± 0.28 ‰ for the uncontaminated Victoria's Lava Lake komatiite melt. For these calculations Monte Carlo simulation (20'000 cycles) was used for error propagation assuming a 10% uncertainty on the initial values where no error estimates have been available.

The very homogeneous $\delta^{98}\text{Mo}$ values within the Victoria's Lava Lake, Pyke Hill and Weltevreden komatiite systems indicate that Mo isotope fractionation during differentiation of these komatiite lavas was very limited. The bulk Mo isotope composition of the komatiite lavas for each of the three localities can therefore be calculated as the average of the samples analyzed. Averaging ($\pm 2\text{SE}$) yields $\delta^{98}\text{Mo} = 0.05 \pm 0.06$ ‰ for Pyke Hill, 0.04 ± 0.04 ‰ for Weltevreden and -0.04 ± 0.28 ‰ for Victoria's Lava Lake. For the Komati locality, the $\delta^{98}\text{Mo}$ of the chilled margin sample BV02 with 0.11 ± 0.10 ‰ (2SD of a single measurement) is used here as our best estimate for the Mo isotopic composition of the emplaced Komati lava.

Although determined with various degree of precision, the obtained Mo isotopic compositions for the four komatiite systems are identical within their respective uncertainties. Averaging Mo isotopic compositions for the four komatiite systems yields a $\delta^{98}\text{Mo}$ of 0.04 ± 0.06 ‰ (2SE, Table 2). This value represents our best estimate for the average Mo isotopic composition of the studied Archean komatiites.

5.3. Molybdenum concentrations and isotope compositions of the komatiite mantle sources

The Mo concentrations in the mantle sources of the studied komatiite systems were estimated using the same projection technique utilized in this study for calculating the Mo concentration of the emplaced komatiite lava. This technique has been applied to calculate the absolute abundances of the incompatible highly siderophile elements (e.g., Pt, Pd, and Re) in the mantle sources of the Pyke Hill (Puchtel et al., 2004a), the lower Komati, and the Weltevreden Formation komatiites (Puchtel et al., 2014). The MgO content of the mantle is only influenced to a minor degree by previous melt extractions and thus, a MgO concentration from 38 to 40 wt%, similar to that in the Bulk Silicate Earth estimates of McDonough and Sun (1995), is assumed for the komatiite mantle sources. The errors were estimated in the same way as for the calculation of the Mo concentration in the emplaced komatiite lavas. Calculations give 30 ± 12 ng/g for Victoria's Lava Lake, 17 ± 5 ng/g for Pyke Hill, 17 ± 3 ng/g for Weltevreden, and 29 ± 7 ng/g for the lower Komati Formation komatiite mantle sources. Averaging all four calculated values (Table 2) yields 23 ± 7 ng/g (2SE), which is our best estimate for the BSE. This value is identical, within the uncertainties, to estimates for Mo concentration in the primitive mantle of 39 ± 16 ng/g (Figure 6) calculated on the basis on an assumed constant Mo/Ce ratio of ~ 0.3 (Palme and O'Neill, 2004).

Due to the high degrees of partial melting, the complete base metal sulfide removal from the mantle melting region, and the high liquidus temperatures of the komatiite lavas, it is assumed in this study that the $\delta^{98}\text{Mo}$ values of the emplaced komatiite lavas closely resemble the Mo isotope compositions of their respective mantle sources. The average of Mo isotope compositions of the mantle sources of the studied komatiites is 0.04 ± 0.06 ‰ (2SE); we consider this $\delta^{98}\text{Mo}$ value as representing the Mo isotope composition of the Bulk Silicate Earth, as defined by the Mo isotopic composition of mantle sources of Archean komatiite systems. This value is indistinguishable from the chondritic $\delta^{98}\text{Mo}$ value of 0.09 ± 0.02 ‰ (Burkhardt et al., 2014) (Figures 2 and 6).

The calculated Mo isotopic composition of the BSE is lighter than the estimated average Mo isotopic composition ($\delta^{98}\text{Mo} = 0.3$ to 0.4 ‰) of the upper igneous continental crust (Voegelin et al., 2014). From the mass-balance standpoint, an isotopically lighter reservoir compared to the BSE must exist in the Earth's mantle. This reservoir could be represented by subducting slabs that are expected to accumulate at either the transition zone, or even the core-mantle boundary (Kerr, 1997, Van der Hilst and Karason, 1999). Incorporation of the material of recycled oceanic crust in mantle plumes may result in lighter Mo isotope composition of some plume lavas.

5.4. Implications for the core-mantle equilibration

It is assumed that late stages of Earth accretion involved collisions of several Moon- to Mars-sized planetary embryos, which were already differentiated into a metallic core and a silicate mantle (e.g., Wood et al., 2006, Stevenson 2008, Rudge et al., 2010). An open discussion exists as to the extent to which the metallic cores of the planetary embryos were equilibrated with the silicate liquid during and after the collisions. If the cores of the planetary embryos were dispersed as metal droplets after the impact, then they should have equilibrated with the silicate mantle at temperatures above 2500°C (e.g., Wood et al., 2006; Siebert et al., 2013), which is the temperature at which Mo isotope fractionation between silicate and metal liquid becomes smaller than the current analytical precision of the Mo isotopic analysis (Hin et al., 2013). If Earth's core formed by merging of several metallic cores without complete equilibration with the silicate portion of the planet, then the Bulk Silicate Earth $\delta^{98}\text{Mo}$ should carry a memory of the core-forming events that happened in the planetary embryos, a process suggested to have occurred at lower temperatures (e.g., Kleine et al., 2009, Rudge et al., 2010 and Stevenson, 2008). That should result in Mo isotopic composition of the terrestrial mantle being distinct from that of the accreted chondritic material. Thus, the most straightforward interpretation of the similarity of Mo isotopic composition between chondritic meteorites, and estimates for the Bulk Silicate Earth from this study is that during the final stages of terrestrial accretion, metal droplets equilibrated with the silicate liquid and the chemical equilibrium between Fe metal of the core and the silicate mantle was essentially achieved.

The results of Mo partitioning experiments under various conditions allow elucidating the temperature and pressure at the time of Earth's core formation. Wade et al. (2012) proposed that the W and Mo composition of the BSE is best explained with sulfur addition during the last 10 to 20% of Earth's core formation. In contrast, based on Mo concentrations only, Burkemper et al. (2012) suggested that the pressures and temperatures during a single stage core forming event must have been between 40-54 GPa and 2775-3125°C (at $f\text{O}_2 = -2.2 \Delta\text{IW}$ and using KLB-1 peridotite composition as a proxy for the silicate melt). This temperature is inline with a chondritic Mo isotope composition of the BSE.

The average chondritic Mo concentration of 1332 ± 430 ng/g (2SD) (Burkhardt et al., 2014) is used to estimate the effect of the addition of late accreted materials constituting 0.5% of the terrestrial

mass (e.g. Mann et al., 2012) on the BSE's Mo inventory. Such an event would have resulted in the addition of 6.7 ± 2.0 ng/g Mo to Earth's early mantle, which corresponds to around 17% or 29%, assuming a post accretion BSE Mo concentration of 39 ng/g (Palme and O'Neill 2004) or 23 ng/g (this study), respectively. Therefore, Mo addition via late accretion did not influence significantly the Mo isotope composition of a mantle with a near chondritic $\delta^{98}\text{Mo}$.

Further studies on Mo isotope fractionation during silicate liquid – metal liquid separation and the influence of sulfur, in combination with a more precisely defined $\delta^{98}\text{Mo}$ of the Bulk Silicate Earth and chondritic meteorites might help better understand the conditions of core formation on Earth and other terrestrial planets.

Acknowledgments

Helen Williams and two unknown reviewers are thanked for their constructive criticism and Bernard Marty is thanked for the editorial handling. Provision of Komati and Weltevreden samples by Gary Byerly and Euan Nisbet to I.S.P. enabling us to use them in this study is gratefully acknowledged. Thomas Pettke is thanked for help with LA-ICP-MS measurements.

References

- Adam, J. and Green, T., 2006, Trace element partitioning between mica- and amphibole-bearing garnet lherzolite and hydrous basanitic melt: 1. Experimental results and the investigation of controls on partitioning behaviour. *Contributions to Mineralogy and Petrology* 152: 1-17.
- Arnold, G.L., Anbar, A.D., Barling, J., Lyons, T.W., 2004. Molybdenum isotope evidence for widespread anoxia in mid-Proterozoic oceans. *Science* 304, 87–90.
- Arndt, N.T., 1976, Melting relations of ultramafic lavas (komatiites) at one atmosphere and high pressure: Year book - Carnegie Institution of Washington, 75, 555–562.
- Arndt, N.T., 1977, Ultrabasic magmas and high-degree melting of the mantle. *Contributions to Mineralogy and Petrology*, v. 64, pp. 205-221
- Arndt N.T., Naldrett A.J. and Pyke D.R., 1977, Komatiitic and iron-rich tholeiitic lavas of Munro Township, northeast Ontario: *Journal of Petrology*, 18, 319–369.
- Arndt, N.T., Kerr, A.C., and Tarney, J., 1997, Dynamic melting in plume heads: the formation of Gorgona komatiites and basalts: *Earth and Planetary Science Letters*, v. 146, no. 1.

510 Baldwin, G.J., Nagler, T.F., Greber, N.D., Turner, E.C., and Kamber, B.S., 2013, Mo isotopic composition of the
511 mid-Neoproterozoic ocean: An iron formation perspective: *Precambrian Research*, v. 230, p. 168–178.

512 Burkemper, L.K., Agee, C.B., and Garcia, K.A., 2012, Constraints on core formation from molybdenum solubility
513 in silicate melts at high pressure: *Earth and Planetary Science Letters*, v. 335-336.

514 Burkhardt, C.N., Hin, R.C., Kleine, T., and Bourdon, B., 2014, Evidence for Mo isotope fractionation in the solar
515 nebula and during planetary differentiation: *Earth and Planetary Science Letters*, v. 391, no. C, p. 201–211.

516 Connolly, B.D., Puchtel, I.S., Walker, R.J., Arevalo, R., Jr., Piccoli, P.M., Byerly, G., Robin-Popieul, C., and Arndt,
517 N., 2011, Highly siderophile element systematics of the 3.3Ga Weltevreden komatiites, South Africa:
518 Implications for early Earth history: *Earth and Planetary Science Letters*, v. 311, no. 3-4, p. 253–263.

519 Dauphas, N., Roskosz, M., Alp, E.E., Neuville, D.R., Hu, M.Y., Sio, C.K., Tissot, F.L.H., Zhao, J., Tissandier, L.,
520 Medard, E., and Cordier, C., 2014, Magma redox and structural controls on iron isotope variations in Earth's
521 mantle and crust: *Earth and Planetary Science Letters*, v. 398, no. C.

522 Farkaš, J., Chrástný, V., Novák, M., Čadkova, E., Pašava, J., Chakrabarti, R., Jacobsen, S.B., Ackerman, L., and
523 Bullen, T.D., 2013, Chromium isotope variations ($\delta^{53/52}\text{Cr}$) in mantle-derived sources and their weathering
524 products: Implications for environmental studies and the evolution of $\delta^{53/52}\text{Cr}$ in the Earth's mantle over
525 geologic time: *Geochimica et Cosmochimica Acta*, v. 123, p. 74–92.

526 Goldberg, T., Gordon, G.W., Izon, G., Archer, C., Pearce, C.R., McManus, J., Anbar, A.D., and Rehkamper, M.,
527 2013, Resolution of inter-laboratory discrepancies in Mo isotope data: an intercalibration: *Journal of Analytical*
528 *Atomic Spectrometry*, doi: 10.1039/c3ja30375f.

529 Greber, N.D., Pettke, T., and Nagler, T.F., 2014, Magmatic–hydrothermal molybdenum isotope fractionation and
530 its relevance to the igneous crustal signature: *Lithos*, v. 190-191, no. C, p. 104–110.

531 Greber, N.D., Siebert, C., Nagler, T.F., and Pettke, T., 2012, $\delta^{98/95}\text{Mo}$ values and Molybdenum Concentration
532 Data for NIST SRM 610, 612 and 3134: Towards a Common Protocol for Reporting Mo Data: *Geostandards*
533 *and Geoanalytical Research*, v. 36, no. 3, p. 291–300.

534 Hin, R.C., Burkhardt, C.N., Schmidt, M.W., Bourdon, B., and Kleine, T., 2013, Experimental evidence for Mo
535 isotope fractionation between metal and silicate liquids: *Earth and Planetary Science Letters*, v. 379, no. C, p.
536 38–48.

537 Keays, R.R., 1995, The role of komatiitic and picritic magmatism and S-saturation in the formation of ore deposits:
538 *Lithos*, v. 34, no. 1, p. 1–189.

539 Kerr, R. A. (1997). Deep-sinking slabs stir the mantle. *Science*, vol. 275, pp. 613-615.

540 Kleine, T., Touboul, M., Bourdon, B., Nimmo, F., Mezger, K., Palme, H., Jacobsen, S.B., Yin, Q.-Z., and Halliday,
541 A.N., 2009, Hf–W chronology of the accretion and early evolution of asteroids and terrestrial planets:
542 *Geochimica et Cosmochimica Acta*, v. 73, no. 17, p. 5150–5188.

543 Li, Y., and Audétat, A., 2012, Partitioning of V, Mn, Co, Ni, Cu, Zn, As, Mo, Ag, Sn, Sb, W, Au, Pb, and Bi
 544 between sulfide phases and hydrous basanite melt at upper mantle conditions: *Earth and Planetary Science*
 545 *Letters*, v. 355-356.

546 Mann, U., Frost, D.J., Rubie, D.C., Becker, H., and Audetat, A., 2012, Partitioning of Ru, Rh, Pd, Re, Ir and Pt
 547 between liquid metal and silicate at high pressures and high temperatures - Implications for the origin of highly
 548 siderophile element concentrations in the Earth's mantle: *Geochimica et Cosmochimica Acta*, v. 84.

549 McDonough, W.F., and Sun, S.S., 1995, The composition of the Earth: *Chemical Geology*, v. 120, no. 3, p. 223-
 550 253.

551 Nägler, T.F., Anbar, A.D., Archer, C., Goldberg, T., Gordon, G.W., Greber, N.D., Siebert, C., Sohrin, Y., and
 552 Vance, D., 2014, Proposal for an International Molybdenum Isotope Measurement Standard and Data
 553 Representation: *Geostandards and Geoanalytical Research*, v. 38, no. 2, p. 149-151.

554 Nisbet E.G., Cheadle M.J., Arndt N.T. and Bickle M.J., 1993, Constraining the potential temperature of the
 555 Archaean mantle: a review of the evidence from komatiites. *Lithos*, v. 30, no. 3-4, p. 291– 307.

556 Oze, C., Bird, D.K., and Fendorf, S., 2007, Genesis of hexavalent chromium from natural sources in soil and
 557 groundwater: *Proceedings of the National Academy of Sciences*, v. 104, no. 16.

558 Palme, H. and O'Neill, H.St.C., 2004, Cosmochemical estimates of Mantle Composition. In: *Treatise on*
 559 *Geochemistry*. Holland, H.D. and Turekian, K.K. (Editors), Elsevier, Amsterdam, The Netherlands. 2: 1-38.

560 Pearce, C.R., Cohen, A.S., Coe, A.L., and Burton, K.W., 2008, Molybdenum isotope evidence for global ocean
 561 anoxia coupled with perturbations to the carbon cycle during the Early Jurassic: *Geology*, v. 36, no. 3, p. 231.

562 Pettke, T., Oberli, F., Audetat, A., Guillong, M., Simon, A., Hanley, J., Klemm, L.M., 2012, Recent developments
 563 in element concentration and isotope ratio analysis of individual fluid inclusions by laser ablation single and
 564 multiple collector ICP–MS, *Ore Geological Reviews* 44, 10–38.

565 Puchtel, I.S., Blichert-Toft, J., Touboul, M., Walker, R.J., Byerly, G.R., Nisbet, E.G., and Anhaeusser, C.R., 2013,
 566 Insights into early Earth from Barberton komatiites: Evidence from lithophile isotope and trace element
 567 systematics: *Geochimica et Cosmochimica Acta*, v. 108, no. C, p. 63–90.

568 Puchtel, I.S., Haase, K.M., Hofmann, A.W., Chauvel, C., Kulikov, V.S., Garbe-Schonberg, C.D., and Nemchin,
 569 A.A., 1997, Petrology and geochemistry of crustally contaminated komatiitic basalts from the Vetryny Belt,
 570 southeastern Baltic Shield: Evidence for an early Proterozoic mantle plume beneath rifted Archean continental
 571 lithosphere: *Geochimica et Cosmochimica Acta*, v. 61, p. 1205–1222.

572 Puchtel, I.S., Humayun, M., Campbell, A.J., Sproule, R.A., and Leshner, C.M., 2004a, Platinum group element
 573 geochemistry of komatiites from the Alexo and Pyke Hill areas, Ontario, Canada: *Geochimica et*
 574 *Cosmochimica Acta*, v. 68, no. 6, p. 1361–1383.

575 Puchtel, I.S., Brandon, A.D., and Humayun, M., 2004b, Precise Pt–Re–Os isotope systematics of the mantle from
576 2.7-Ga komatiites: *Earth and Planetary Science Letters*, v. 224, no. 1-2, p. 157–174.

577 Puchtel, I.S., Hofmann, A.W., Mezger, K., Shchipansky, A.A., Kulikov, V.S., and Kulikova, V.V., 1996, Petrology of
578 a 2.41 Ga remarkably fresh komatiitic basalt lava lake in Lion Hills, central Vetryny Belt, Baltic Shield:
579 *Contributions to Mineralogy and Petrology*, v. 124, p. 273–290.

580 Puchtel, I.S., Touboul, M., Walker, R.J., Blichert-Toft, J., Brandon, A.D., Kulikov, V.S., and Samsonov, A.V., (in
581 prep). Lithophile and siderophile element systematics of the mantle at the Archean-Proterozoic boundary:
582 Evidence from 2.4 Ga komatiites. *Geochimica et Cosmochimica Acta* (in preparation).

583 Puchtel, I.S., Walker, R.J., Touboul, M., Nisbet, E.G., and Byerly, G.R., 2014, Insights into early Earth from the Pt-
584 Re-Os isotope and highly siderophile element abundance systematics of Barberton komatiites: *Geochimica et*
585 *Cosmochimica Acta*, v. 125, no. C, p. 394–413.

586 Rudnick, R.L., and Gao, S., 2003, 3.01 - Composition of the Continental Crust: In *Treatise on Geochemistry*
587 (Second Edition), eds. Holland, H.D., and Turekian, K.K., Elsevier, Oxford, v. 3, p. 1–64.

588 Rudge, J.F., Kleine, T., and Bourdon, B., 2010, Broad bounds on Earth's accretion and core formation
589 constrained by geochemical models: *Nature Geoscience*, v. 3, no. 6, p. 439–443.

590 Siebert, J., Badro, J., Antonangeli, D., and Ryerson, F.J., 2013, Terrestrial Accretion Under Oxidizing Conditions:
591 *Science*, v. 339, no. 6124, p. 1194–1197.

592 Stevenson, D.J., 2008, A planetary perspective on the deep Earth: *Nature*, v. 451, no. 7176, p. 261–265.

593 Van der Hilst, R. D. and Karason, H. (1999). Compositional heterogeneity in the bottom 1000 kilometers of Earth's
594 mantle: Toward a hybrid convection model. *Science*, vol. 283, pp. 1885-1888.

595 Voegelin, A.R., Nägler, T.F., Pettke, T., Neubert, N., Steinmann, M., Pourret, O., and Villa, I.M., 2012, The impact
596 of igneous bedrock weathering on the Mo isotopic composition of stream waters: Natural samples and
597 laboratory experiments: *Geochimica et Cosmochimica Acta*, v. 86, p. 150–165.

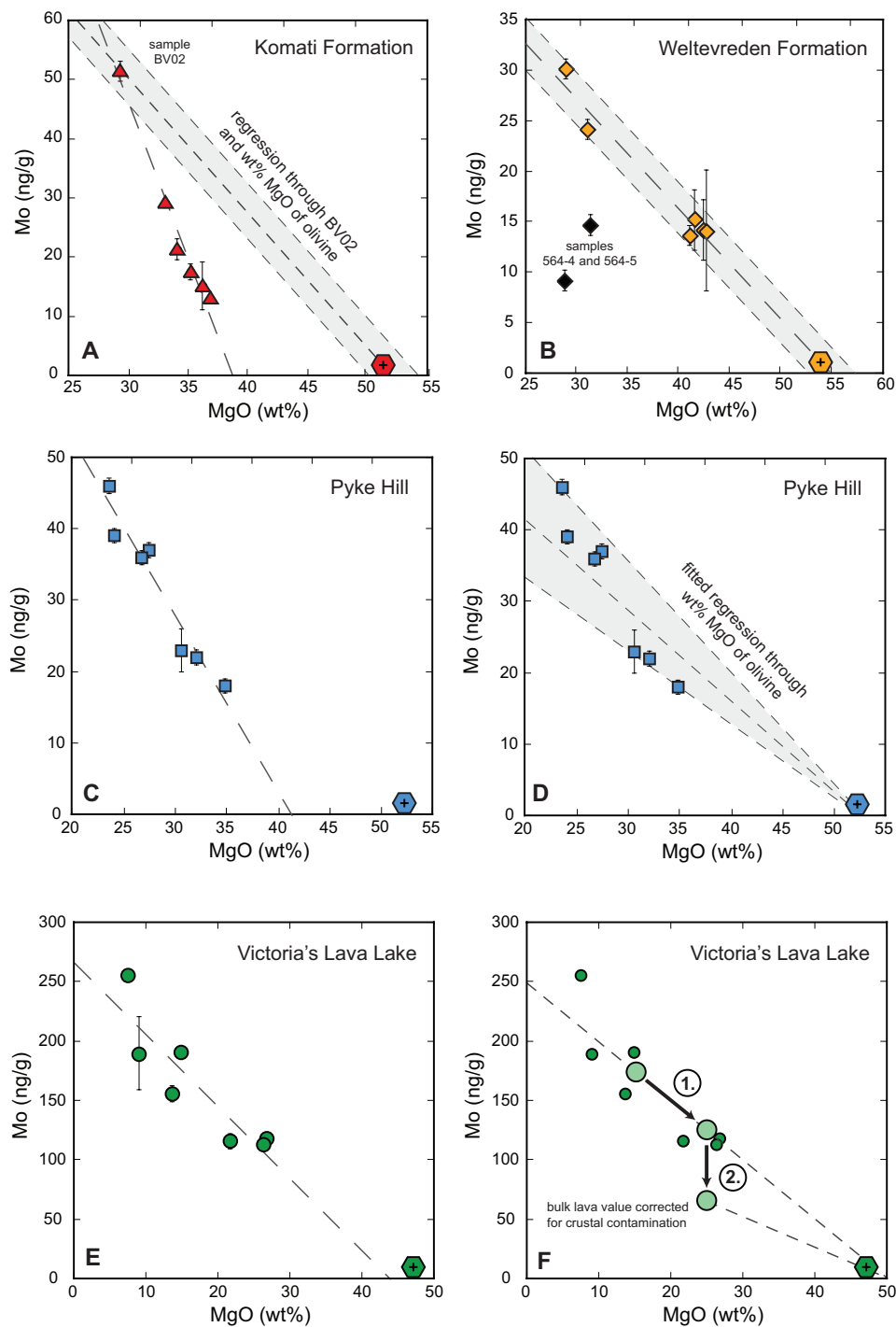
598 Voegelin, A.R., Pettke, T., Greber, N.D., Niederhäusern, von, B., and Nägler, T.F., 2014, Magma differentiation
599 fractionates Mo isotope ratios: Evidence from the Kos Plateau Tuff (Aegean Arc): *Lithos*, v. 190-191, p. 440–
600 448.

601 Wille, M., Kramers, J.D., Nägler, T.F., Beukes, N.J., Schröder, S., Meisel, T., Lacassie, J.P., and Voegelin, A.R.,
602 2007, Evidence for a gradual rise of oxygen between 2.6 and 2.5 Ga from Mo isotopes and Re-PGE
603 signatures in shales: *Geochimica et Cosmochimica Acta*, v. 71, p. 2417.

604 Wade, J., Wood, B.J., and Tuff, J., 2012, Metal-silicate partitioning of Mo and W at high pressures and
605 temperatures: Evidence for late accretion of sulphur to the Earth: *Geochimica et Cosmochimica Acta*, v. 85.

606 Wood, B.J., Walter, M.J., and Wade, J., 2006, Accretion of the Earth and segregation of its core: *Nature*, v. 441,
607 no. 7095, p. 825–833,

609 **Figures**



610

611 **Figure 1:** Variation diagrams of Mo vs. MgO for the investigated komatiite systems (A,B,C and E). Best estimates

612 of liquid lines of descents (A, D) and correction for crustal contamination (F) are indicated. For explanation of used

613 regressions (A, D) and different steps to correct for crustal contamination (F), see text. Samples 564-4 and 564-5

614 of the Weltevreden suite (B) have been omitted for liquid line of descent. Hexagons show the MgO concentration

615 of olivine from the literature. MgO concentrations of samples and olivine are from Puchtel et al. (1996, 2004a,

616 2013).

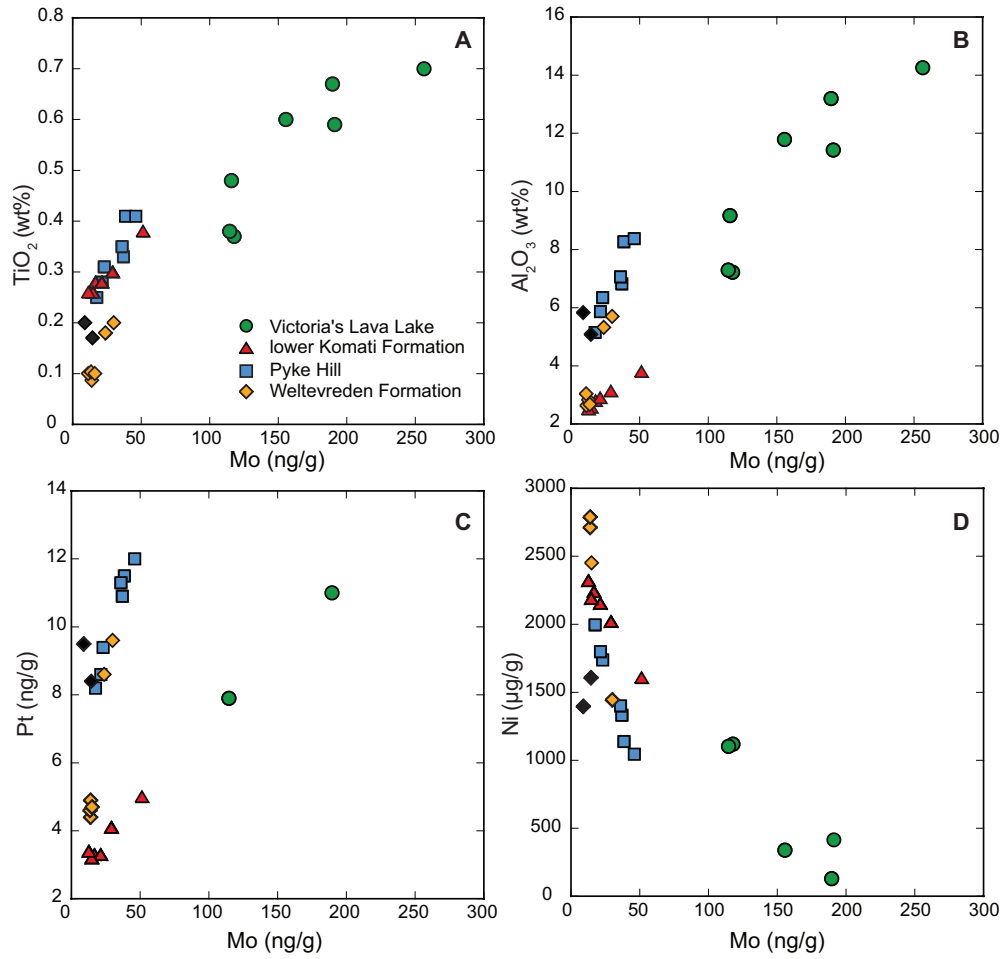


Figure 2: Variation diagrams for TiO₂, Al₂O₃, Pt, and Ni vs Mo concentrations. Mo concentrations show positive correlations with elements incompatible (TiO₂, Al₂O₃, Pt) and negative with elements compatible (Ni) in olivine. Major and trace element data are published in Puchtel et al. (1996, 2001, 2004a, 2013, 2014). Black Weltevreden symbols are samples 564-4 and 564-5 that have been omitted for liquid line of descent (see Figure 1 and text).

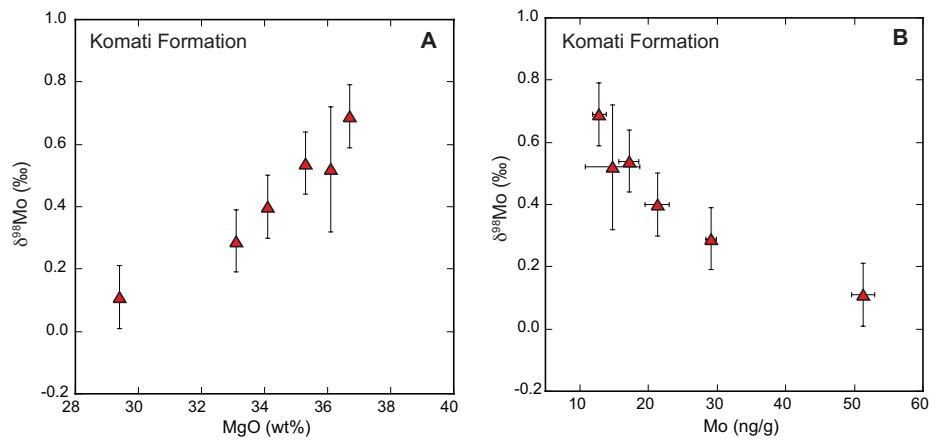
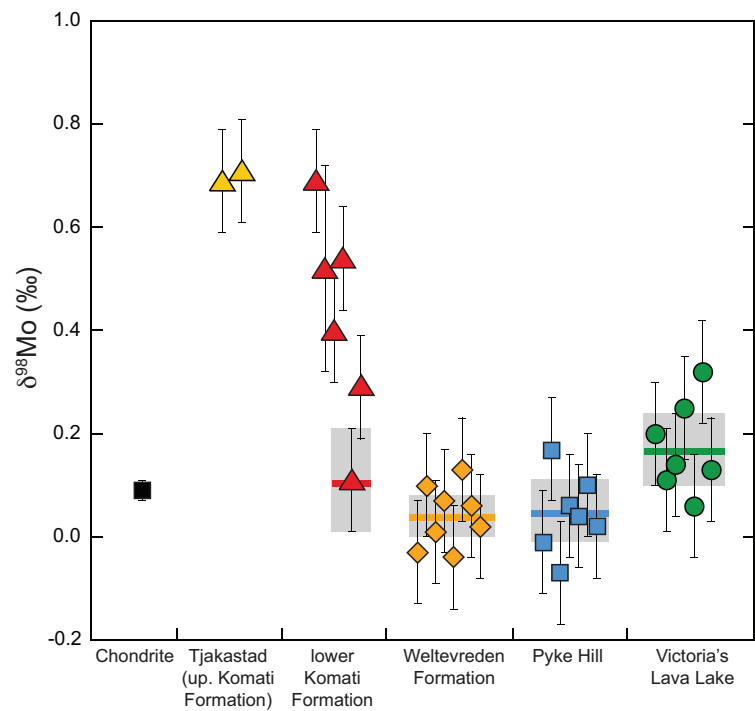


Figure 3: Variation diagrams for $\delta^{98}\text{Mo}$ vs. MgO (A) and Mo (B), for the lower Komati Formation komatiites only. The Mo isotope compositions in these system correlate well with the MgO and the Mo concentrations and show variation up to 0.60‰.



629

630

631

632

633

634

635

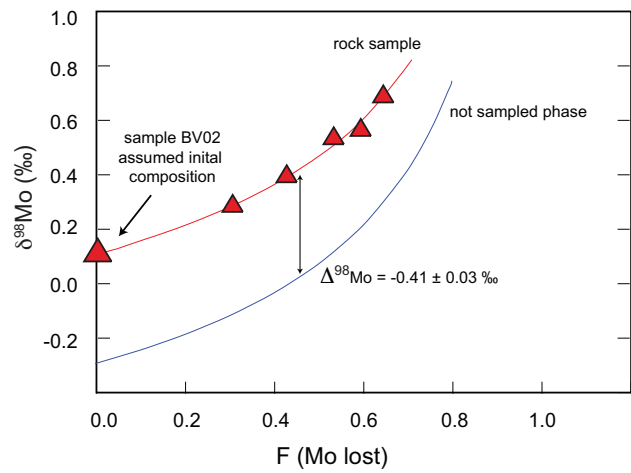
636

637

638

Figure 4: Summary of $\delta^{98}\text{Mo}$ data. Colored lines with grey bars represent bulk Mo isotope composition of the emplaced komatiite lavas. The Mo isotope composition of komatiites from Weltevreden, Pyke Hill and Victoria's Lava Lake (not corrected for crustal contamination, see text) are very homogeneous and similar to the proposed composition of enstatite and ordinary chondrites. The $\delta^{98}\text{Mo}$ of the lower Komati Formation komatiites display a large range with the most strongly altered samples from Tjakastad (upper Komati Formation) having the heaviest Mo isotope composition. Errors on single measurements are 2SD of the standard reproducibility (i.e. 0.1‰, see text). Errors on the displayed average data are 2SE except for Komati Formation (2SD on single measurement). $\delta^{98}\text{Mo}$ of chondrite is from Burkhardt et al. (2014).

639



640

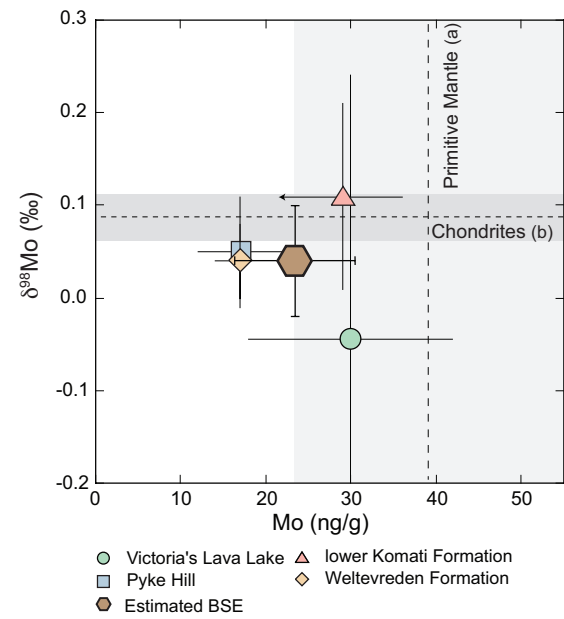
641

642

643

644

Figure 5: Modeled Rayleigh distillation for the Mo isotope variation among the lower Komati Formation, assuming Mo loss after lava eruption for the samples that plot below the liquid line of descent indicated in Figure 1A. For errors on $\delta^{98}\text{Mo}$ see Figure 3 or Table 1.



645

646

647

648

649

650

651

652

Figure 6: Mo concentration of the komatiite mantle sources vs Mo isotope composition. Data is compared to literature data (dotted lines = averages) and shows similarity between suggested Mo concentrations of the primitive mantle (a: Palme and O'Neill 2004) and chondritic $\delta^{98}\text{Mo}$ (b: Burkhardt et al., 2014). The arrow on the error bar for sample from the lower Komati Formation indicates that its Mo concentration is a maximum estimate. Mo signature for Victoria's Lava Lake is corrected for crustal contamination. Error calculations are described in the text.

653 Table 1: Molybdenum concentration and isotope composition data

Sample	Location	Facies	$\delta^{98}\text{Mo}$ ‰				[Mo] ng/g			
			a	b	Average	2SD ^B	a	b	Average	2SD
01110/1	Victoria's Lava Lake	FB	0.09	0.17	0.13	0.10	193	190	191	4
01111		CM	0.29	0.35	0.32	0.10	158	153	156	7
91101		Sp	0.17	0.23	0.20	0.10	201	178	190	31
01001_A		OC	n.a	0.25	0.25	0.10	118	120	118	3
01105		OC	0.13	0.15	0.14	0.10	114	115	114	2
12124		Basalt	0.16	0.05	0.11	0.10	257	256	256	1
12106		OC	0.01	0.11	0.06	0.10	120	116	116	6
K04	Vodla Block	Tonalite	0.21	0.25	0.23	0.10	16	13	16	4
K13		Tonalite	-0.10	-0.05	-0.08	0.10	47	45	47	3
PH13	Pyke Hill	Sp	0.01	0.03	0.02	0.10	39	38	39	1
PH14		Sp	0.10	-	0.10	0.10	46	-	46	1
PH26		Sp	0.04	-	0.04	0.10	37	-	37	1
PH27		Sp	0.06	-	0.06	0.10	36	-	36	1
PH29		OC	-0.03	-0.10	-0.07	0.10	24	22	23	3
PH31		OC	0.19	0.15	0.17	0.10	17	18	18	1
PH33		OC	0.01	-0.03	-0.01	0.10	22	21	22	1
501-1	Weltevreden Formation	OC	n.a	0.02	0.02	0.10	16	12	14	6
501-3		Sp	n.a	0.06	0.06	0.10	24	24	24	1
501-8		OC	n.a	0.13	0.13	0.10	15	13	14	3
427-5		OC	n.a	-0.04	-0.04	0.10	14	13	14	1
564-4		Sp	0.07	n.a.	0.07	0.10	9	9	9	1
564-5		Sp	0.09	-0.08	0.01	0.10	15	14	15	1
12-2		Sp	0.10	-	0.10	0.10	30	-	30	1
12-7		OC	n.a	-0.03	-0.03	0.10	16	14	15	3
BV01	lower Komati Formation	OC	0.37	0.22	0.29	0.10	29	29	29	1
BV02		CM	0.08	0.13	0.11	0.10	51	52	51	2
BV03		OC	n.a	0.54	0.54	0.10	17	18	17	1
BV10		OC	0.38	0.41	0.4	0.10	22	21	21	2
BV13 ^A		OC	0.66	0.37	0.52	0.20	13	16	15	4
BV15		OC	0.71	0.68	0.69	0.10	13	12	13	1
Tjakastad-1	upper Komati Formation	Sp	0.73	0.69	0.71	0.10	81	83	82	3
Tjakastad-2		Sp	0.69	-	0.69	0.10	81	-	81	2
SDO-1	USGS Rock standard		1.07 ± 0.05 (2SD; n=5)							

654 Facies: FB= flow top breccia; CM= chilled margin; Sp= spinifex; OC= olivine cumulate

655 A: Not reproduced sample, 2SD of $\delta^{98}\text{Mo}$ longterm reproducibility is doubled

656 B: $\delta^{98}\text{Mo}$ reproducibility of reference standard $\leq \pm 0.10\%$ (2SD) see text and Greber et al., (2012)

657 Mo concentrations are recalculated on an anhydrous basis using LOI from literature (Puchtel et al., 1996; Puchtel et al., 2004a;
658 Puchtel et al., 2013)

659 Accuracy of single Mo ID concentration measurements is $\pm 2\%$ (Greber et al., 2012) and is applied for samples that were
660 measured only once

661 n.a: not available due to wrong sample-spike ratio or too low Mo signal

663 Table 2: Summary of estimated Mo concentrations and isotope compositions of emplaced komatiites,
664 mantel sources and the Bulk Silicate Earth

	Mo (ng/g)		$\delta^{98}\text{Mo}$ (‰)
	Emplaced lava	Mantle source	
Victoria's Lava Lake ^A	66 ± 22	30 ± 12	-0.04 ± 0.28
Pyke Hill	33 ± 8	17 ± 5	0.05 ± 0.06
Weltevreden	25 ± 4	17 ± 3	0.04 ± 0.04
lower Komati Formation	51 ± 6	29 ± 7	0.11 ± 0.10
Estimated BSE ^B		23 ± 7	0.04 ± 0.06

665 A: Corrected for crustal contamination (see text)

666 B: Errors are 2SE

667